NASA TN D-222

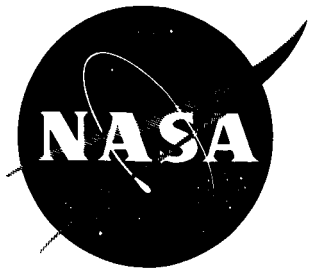

TECHNICAL NOTE
D-222

AN INVESTIGATION OF THE ROLE OF GASEOUS DIFFUSION IN THE OXIDATION OF A METAL FORMING A VOLATILE OXIDE

By Jerry L. Modisette and David R. Schryer

Langley Research Center
Langley Field, Va.

NATIONAL AERONAUTICS AND SPACE ADMINISTRATION

WASHINGTON

March 1960

ERRATA

NASA Technical Note D-222

By Jerry L. Modisette and David R. Schryer
March 1960

Page 8: Equation (14) should read as follows:

$$k_{av} = \frac{2PDC_\infty}{5\left(\frac{\mu l}{\rho u_\infty}\right)^{1/2}}\left\{1 - \frac{4PD}{5\left(\frac{\mu l}{\rho u_\infty}\right)^{1/2}\bar{V}\exp\left(\frac{-E_a}{RT}\right)}\log_e\left[1 + \frac{5\left(\frac{\mu l}{\rho u_\infty}\right)^{1/2}\bar{V}\exp\left(\frac{-E_a}{RT}\right)}{4PD}\right]\right\} \qquad (14)$$

Pages 14-18 and 22-24: The values of u_∞ given in table I and in the sublegends of figures 3 and 4 should be multiplied by 4.

Page 19: The values of P given in table II should be divided by 2.

NASA-Langley, 1962

Issued 1-4-62

NATIONAL AERONAUTICS AND SPACE ADMINISTRATION

TECHNICAL NOTE D-222

AN INVESTIGATION OF THE ROLE OF GASEOUS DIFFUSION IN THE OXIDATION OF A METAL FORMING A VOLATILE OXIDE

By Jerry L. Modisette and David R. Schryer

SUMMARY

A theoretical analysis of the oxidation of a metal forming a volatile oxide has been made which takes into consideration gaseous diffusion of oxygen to the surface and an activated reaction at the surface. The result is a rate equation which expresses oxidation rate as a function of temperature, gas properties, flow conditions, and the activation energy at temperatures at which the oxide is gaseous. The oxidation rate of one such metal, molybdenum, was measured in flowing streams of air and helium-oxygen mixtures at temperatures of 1945° R to 2959° R and flow velocities of 1.2 to 6.5 feet per second. The oxidation rate was found to increase with increasing temperature, flow velocity, and diffusivity in agreement with the results of the analysis. The simple Arrhenius plot was found to give large variations in the values of the activation energy at temperatures above 2400° R for the various experimental conditions. The new rate equation considering gaseous diffusion yielded activation energy values in good agreement with each other. The average value of the activation energy from the new rate equation is 38.3×10^{3} British thermal units per pound-mole of oxygen consumed.

INTRODUCTION

Because of the high temperatures associated with high-speed flight, an increasing need has arisen for structural materials having melting points and good strength characteristics above the 2500° to 3000° R limit of the commonly used iron-nickel-chromium-cobalt alloys. Three classes of structural materials are frequently characterized by high melting points: ceramics, intermetallic compounds, and metals. Both from the standpoint of strength-to-weight ratios and fabrication difficulties, it is desirable to construct the mass of an airframe from metals and alloys.

There are six metals - tungsten, tantalum, molybdenum, niobium, zirconium, and titanium - having melting points significantly above 3000° R which are in sufficient supply and for which fabrication techniques

have been so developed as to allow their use as major structural components. (See ref. 1.) Each of these metals has acceptable strength properties somewhat above 3000° R in the absence of an oxidizing atmosphere. However, the earth has an oxidizing atmosphere and exposure of a metal of this group to air causes failure at temperatures at which the metal would still be otherwise satisfactory. The oxidation deteriorates the metal either by removal of large amounts of structural mass through formation of the oxide (tungsten, molybdenum), weakening the metal by affecting the crystalline properties (zirconium, titanium), or a combination of the two effects (tantalum, niobium).

It is clear that, if the temperature range at which structures can function usefully is to be extended beyond present limitations, it will be necessary to cope with the problem of oxidation. A logical first step toward coping with this problem is to study the physical process involved.

It has been found that at a given temperature the oxidation mechanism for most metals is largely determined by the physical properties of the oxide formed. For most metals for which oxidation studies have been made, the oxide is a solid at all temperatures below the melting point of the metal and it has developed that, in such cases, the transport of the oxygen through the protective solid oxide is usually so much slower than any other steps involved that it constitutes the sole rate-determining factor.

However, some metals (for example, tungsten, tantalum, molybdenum, and niobium) form oxides that melt or vaporize below the melting points of the underlying metals. It might be expected, therefore, that the oxidation of one of these metals in the temperature range at which its oxide is not solid would proceed by a somewhat altered mechanism. In particular, it might be expected that, if the temperature is sufficiently high to vaporize the oxide as rapidly as it is formed, the protection afforded the metal surface by the oxide would be meager and have little influence on the rate of oxidation. Since the unprotected metal surface would be vulnerable to direct attack by oxygen, the rate of oxidation would be a function of the concentration of oxygen in the gas at the surface and the diffusion of fresh quantities of oxygen to the surface could become the rate-controlling factor.

The purpose of this investigation was to study the oxidation of metals forming volatile oxides and, in particular, to determine the effects of gaseous diffusion on the rate of oxidation of one such metal, molybdenum. Molybdenum was chosen as the subject of the experimental phase of this investigation because the oxide vaporizes at temperatures facilitating laboratory investigation. The results of this investigation have application to the metals previously mentioned as well as to carbon,

all of which are of interest either as primary structural materials or as protective coatings.

The experimental technique employed was the oxidation of molybdenum in a flowing stream of an oxidizing gas mixture. Weight-loss measurements were made to determine the oxidation rate. Since the rate of diffusion of oxygen to the surface is dependent upon the diffusivity and the rate of flow, these parameters were varied to determine whether such variations produced corresponding variations in the oxidation rate. The variation in diffusivity was achieved by using mixtures of oxygen and helium in addition to air (which is essentially an oxygen-nitrogen mixture). The temperature range covered was 1900° R to 3000° R and the flow velocities varied from 1 to 7 feet per second.

The experimental investigation was complemented by a theoretical analysis of the physical process, which assumed a mechanism involving diffusion of the oxygen through the surrounding gas mixture to the metal surface and activated reaction at the surface.

SYMBOLS

A	collision rate of reacting molecules, $lb\text{-}ft^{-2}\text{-}sec^{-1}$
C	concentration of oxygen
C_o	concentration of oxygen at surface, $lb\text{-}ft^{-3}$
C_∞	free-stream oxygen concentration, $lb\text{-}ft^{-3}$
D	gaseous diffusivity, $ft^2\text{-}sec^{-1}$
E_a	activation energy, $Btu\text{-}(lb\text{-}mole)^{-1}$
k	oxidation rate at a point on a surface, $lb\text{-}ft^{-2}\text{-}sec^{-1}$
k_{av}	average oxidation rate over a surface, $lb\text{-}ft^{-2}\text{-}sec^{-1}$
R	universal gas constant, $Btu\text{-}(lb\text{-}mole)^{-1}\text{-}{}^{o}R^{-1}$
T	absolute temperature, ^{o}R
$\bar{V}$	mean velocity of oxygen molecules, $ft\text{-}sec^{-1}$
P_1	ratio of concentration gradient at surface to average gradient through concentration boundary layer, dimensionless

P_2 ratio of concentration boundary-layer thickness to velocity boundary-layer thickness, dimensionless

$P = \frac{P_1}{P_2}$, dimensionless

l length of plate, ft

x distance from leading edge, ft

y coordinate normal to surface, ft

μ viscosity, slugs-ft^{-1}-sec^{-1}

ρ density, slugs-ft^{-3}

u_∞ free-stream gas velocity, ft-sec^{-1}

δ_c concentration boundary-layer thickness, ft

$\left(\frac{\partial C}{\partial y}\right)_0$ concentration gradient at the surface

THEORETICAL DEVELOPMENT

Diffusion of Oxygen Through Boundary Layer and Activated Reaction at Surface

From the collision theory of absolute reaction rates (ref. 2), the rate of a chemical reaction is given by the integrated form of the Arrhenius equation

$$k = A \exp\left(\frac{-E_a}{RT}\right) \tag{1}$$

The right-hand side of this equation may be thought of as the product of a physical and a chemical factor. The physical factor A is essentially the collision rate of the reacting molecules which, for the case under consideration, is assumed to be equal to the rate at which the oxygen molecules strike the metal surface and the chemical factor $\exp \frac{-E_a}{RT}$ is essentially the fraction of the collisions resulting in

reaction. The activation energy E_a is the minimum energy required for a collision to result in chemical reaction and is a constant for a given reaction and a particular reaction mechanism. In general, a theoretical determination of the activation energy is beyond the present limitations of theoretical chemistry and an experimental determination is required. The collision rate, however, is more amenable to theoretical analysis. Such an analysis for an oxidizing metal surface situated in a flowing gas stream follows.

A second equation for the oxidation rate may be obtained by considering diffusion since for steady-state conditions the oxidation rate will be very nearly equal to the rate of diffusion of oxygen through the gas to the surface.

$$k \approx D\left(\frac{\partial C}{\partial y}\right)_o \tag{2}$$

The equality sign would hold in equation (2) except for a slight suction at the surface caused by a discrepancy between the number of oxygen molecules reacting and the number of oxide molecules produced. This suction causes a mass flow normal to the surface which influences the transport of oxygen. However, this effect is small and is neglected in this paper.

The unknown quantities in equations (1) and (2) are A and $\left(\frac{\partial C}{\partial y}\right)_o$. If it were possible to express these quantities in terms of a common unknown, that unknown could be eliminated from the two equations. Fortunately, with the help of a simplifying assumption, this may be done.

The flow of a gas stream over a metal surface gives rise to an aerodynamic boundary layer. Since oxygen is consumed at the surface, there is also a concentration boundary layer. If the concentration gradient at the surface is assumed to be proportional to the average gradient through the concentration boundary layer,

$$\left(\frac{\partial C}{\partial y}\right)_o = P_1\left(\frac{C_\infty - C_o}{\delta_c}\right) \tag{3}$$

Substituting equation (3) into equation (2) yields

$$k = P_1 D\left(\frac{C_\infty - C_o}{\delta_c}\right) \tag{4}$$

Now C_o is the unknown quantity. The collision rate A is also a function of C_o since from kinetic theory of gases the collision rate of the oxygen molecules with the surface is

$$A = \frac{C_o \bar{V}}{4} \tag{5}$$

Therefore, equation (1) becomes

$$k = \frac{C_o \bar{V}}{4} \exp\left(\frac{-E_a}{RT}\right) \tag{6}$$

By eliminating C_o between equations (4) and (6), an equation is obtained relating oxidation rate to physical properties which are themselves independent of the oxidation rate.

$$k = \frac{\dfrac{P_1 D}{\delta_c} \dfrac{\bar{V} C_\infty}{4} \exp\left(\dfrac{-E_a}{RT}\right)}{\dfrac{\bar{V}}{4} \exp\left(\dfrac{-E_a}{RT}\right) + \dfrac{P_1 D}{\delta_c}} \tag{7}$$

Equation (7) and its derivation are similar to that of Carpenter (ref. 3) except for the introduction of the concept of an activated reaction (a reaction requiring a certain minimum energy, the activation energy) at the surface.

From a comparison of equations (6) and (7), it is obvious that

$$C_o = \frac{\dfrac{P_1 D C_\infty}{\delta_c}}{\dfrac{\bar{V}}{4} \exp\left(\dfrac{-E_a}{RT}\right) + \dfrac{P_1 D}{\delta_c}} \tag{8}$$

It is of interest to note that the derived expression for C_o is a function of the activation energy. This fact becomes important in the experimental determination of the activation energy, as is discussed subsequently in the section "Results and Discussion."

Equation (7) may be used to evaluate the relative importance of the diffusion step when all the physical parameters are known. The denominator of the right-hand side consists of two terms, $\frac{\bar{V}}{4} \exp\left(\frac{-E_a}{RT}\right)$ and $\frac{P_1 D}{\delta_c}$,

the relative size of which determines the relative importance of the diffusion step and the activated reaction step. This may best be seen by considering the limiting cases. If $\frac{\overline{V}}{4} \exp \frac{-E_a}{RT} \gg \frac{P_1 D}{\delta_c}$, then

$$k \approx \frac{P_1 D C_\infty}{\delta_c} \tag{9}$$

This is the case in which the oxygen reacts with the surface as fast as it can diffuse through the boundary layer and thus effectively maintains zero oxygen concentration at the surface.

The second limiting case occurs when $\frac{\overline{V}}{4} \exp\left(\frac{-E_a}{RT}\right) \ll \frac{P_1 D}{\delta_c}$ and thus

$$k \approx \frac{\overline{V} C_\infty}{4} \exp\left(\frac{-E_a}{RT}\right) \tag{10}$$

This is the case in which the diffusion process is so rapid that the reaction of oxygen with the surface causes no appreciable decrease in the oxygen concentration at the surface.

It would be desirable in the interest of simplicity to work always with one of the limiting cases but, of course, this is not always possible. However, the ratio of the terms $\frac{\overline{V}}{4} \exp\left(\frac{-E_a}{RT}\right)$ and $\frac{P_1 D}{\delta_c}$ does afford a criterion, as shown above, for determining when such simplification may be made and which, if either, limiting case applies. If the two terms are of approximately the same size, however, the complete rate equation must be used.

Average Oxidation Rate of Flat Plate in Laminar Flow

The specimens, which were the subject of the experimental investigation were thin flat plates, the total weight losses of which were measured to determine the average oxidation rates over the surface. In order to permit correlation of the preceding analysis with experiment, an expression is derived which is essentially an extension of equation (7) for the special case of the average oxidation rate of a flat plate in laminar flow.

The average oxidation rate of a flat plate of length l is given by the mean value theorem to be

$$k_{av} = \frac{1}{l} \int_0^l k \, dx \tag{11}$$

The only term in the expression for k (eq. (7)) that is a function of x is δ_c. It is assumed that the concentration boundary-layer thickness is proportional to the velocity boundary-layer thickness. If the expression for the boundary-layer thickness given in reference 4 is used,

$$\delta_c = 5P_2\left(\frac{\mu x}{\rho u_\infty}\right)^{1/2} \tag{12}$$

Eliminating k and δ_c between equations (7), (11), and (12) yields

$$k_{av} = \int_0^l \frac{PDC_\infty \, dx}{5\left(\frac{\mu x}{\rho u_\infty}\right)^{1/2} + \frac{4PD}{\overline{V} \exp\left(\frac{-E_a}{RT}\right)}} \tag{13}$$

Integration of equation (13) yields

$$k_{av} = \frac{2PD}{5\left(\frac{\mu l}{\rho u_\infty}\right)^{1/2}} \left\{ 1 - \frac{4PD}{5\left(\frac{\mu l}{\rho u_\infty}\right)^{1/2} \overline{V} \exp\left(\frac{-E_a}{RT}\right)} \log_e \left[1 + \frac{5\left(\frac{\mu l}{\rho u_\infty}\right)^{1/2} \overline{V} \exp\left(\frac{-E_a}{RT}\right)}{4PD} \right] \right\} \tag{14}$$

APPARATUS AND TESTS

Apparatus

Figure 1 shows the experimental facility which is essentially a vertical tube furnace into which the molybdenum specimen can be suspended from the weighing arm of a torsion balance. Provision is made for a metered flow of air or a helium-oxygen mixture through the tube. The furnace tube is of aluminum oxide, 1 inch inside diameter, 30 inches long. A 12-inch section of the tube is heated by silicon carbide resistance elements. The balance is a torsion-spring type with a sensitivity of 0.1 milligram. The balance is situated on top of the furnace and is protected from the heat by a water-cooled baffle.

Temperature was measured by a thermocouple (platinum - platinum, 13-percent rhodium) placed immediately below the test specimen. Tests were made with the thermocouple attached to the specimen and the temperature variation from the bare thermocouple was noted to be 5° R.

The maximum Reynolds number in the tube was calculated to be 150 based on tube diameter; therefore, the flow was assumed to be laminar.

Test Specimens

Each specimen was sheared from 0.010-inch sintered molybdenum sheet and was approximately 0.5 inch by 1.0 inch. Table I gives the exact dimensions of each specimen. The specimen was suspended from a platinum hook through a 1/32-inch-diameter hole drilled 1/16 inch from the center of one of the 0.5-inch edges.

The molybdenum used for all tests reported herein was commercially pure. No analysis of the impurities present was available. A few tests were made with arc-cast molybdenum which was known to be considerably less pure than the sintered molybdenum but no difference was found in the oxidation rate. The specimens were not cleaned or treated in any way prior to testing.

Gas Mixtures

The helium-oxygen mixtures were used in conjunction with air to determine the effect of diffusivity on the oxidation rate. The diffusivity of oxygen in helium is about twice that of oxygen in air. The diffusivities were calculated from the Gilliland equation. (See refs. 5 and 6.) The gases were supplied from commercial cylinders and were not dried before use. Reference 7 indicates that the presence of water vapor has no effect on the oxidation rate of molybdenum.

Tests

The tests were made in five series with each series at a constant mass-flow rate and with a given gas mixture but over a range of temperature. For each test the weight of the specimen and supporting platinum wire was measured at intervals of about 10 to 20 seconds. Weight measurements were not begun until the specimen reached the temperature of the furnace. The temperature and mass-flow rates of the oxidizing gas mixtures were monitored continually during the runs. The average flow velocities across the center 1/2 inch of the tube were calculated from the mass-flow rates and temperatures by assuming a parabolic velocity distribution.

The weight losses were plotted against the elapsed time from the first weight measurement and the oxidation rates were determined from the slopes of the resulting linear plots, representative examples of which are given in figure 2. Table I gives the times, weight measurements, flow velocities, gas compositions, and weight loss rates of each test, grouped according to series.

RESULTS AND DISCUSSION

The data presented in figures 3 to 5 indicate three oxidation regimes with transition temperatures between the regimes at about 2100° R and 2400° R. These temperatures correspond roughly to the melting and boiling points of the trioxide, 1922° R and 2560° R. (See ref. 7.) If the lower transition is assumed to be caused by melting of the oxide, the discrepancy in temperatures may be caused by the presence of other oxides in addition to MoO_3.

The upper transition temperature varies considerably among the different series and tends to decrease with the increase of factors promoting mass transfer (diffusivity, flow velocity). It is believed that the upper transition corresponds to the temperature at which the liquid oxide changes from a macroscopic layer to a submicroscopic layer, that is, the oxide vaporizes as rapidly as it is formed. This condition was observed to be true for series 2 and 3. For these series liquid oxide was observed up to 2400° R. Above this temperature the specimens exhibited a highly polished appearance with no oxide visible. No observations of the surface conditions were made for the other series.

The activation energy for the oxidation of molybdenum was calculated for each series by use of equation (14). Points were taken at two different temperatures (above 2400° R) from each of the faired curves in figures 3 and 4 and substituted into equation (14) to give two equations in P and E_a for each series. Each of the five pairs of equations was solved simultaneously for P and E_a to give five independent experimental determinations of the activation energy, the values of which are given in table II. The values of E_a agree very well with a mean deviation from the average of 3.6 percent. Only the upper regime was considered because this is the only regime to which the equation is strictly applicable.

The activation energy of each series was also determined by means of the simple Arrhenius plot. The plots are given in figure 5 and the values obtained are listed in table II along with the mean variation from the average for each regime. For the two regimes above about 2100° R,

there is large variation in the values. For the upper regime the variation is 17.4 percent.

It is of interest to note that values obtained for the activation energy in the intermediate regime by the simple Arrhenius plot are much lower than those usually associated with high-temperature chemical reactions and their physical significance is questionable.

It is apparent from a comparison of the curves for oxidation rate plotted against temperature presented in figures 3 and 4 that, in the temperature range considered, the rate of oxidation of molybdenum is not a constant at a given temperature but increases with increasing flow velocity and gaseous diffusivity. This result is in agreement with the results of the theoretical analysis.

For example, if the upper regimes of series 2 and 3 are considered (figs. 3(b) and 3(c)), a 37-percent increase in flow velocity produces an 8-percent increase in oxidation rate at the same temperature. A 9-percent increase is predicted by equation (14), the form of the rate equation applicable to the data.

The effect of diffusivity may best be seen by comparing series 4 (fig. 4(a); mixture of 21.5-percent O_2 and 78.5-percent He) and series 3 (fig. 3(c); air) which represent approximately equal flow rates but considerably different diffusivities. It can be seen that a 110-percent increase in diffusivity produces a 38-percent increase in oxidation rate. Equation (14) predicts a 44-percent increase.

Since the flow velocity and diffusivity are factors that govern gaseous diffusion, the fact that they influence the oxidation rate establishes that gaseous diffusion is a rate-controlling step.

The poor agreement in the Arrhenius plot values for the activation energy for various test conditions casts considerable doubt on the validity of such values for diffusion-controlled reactions. This lack of agreement is attributed to the fact that figure 5 is a plot of the logarithm of the absolute reaction rate against $1/RT$; whereas rigorously, the ordinate of the Arrhenius plot should be the logarithm of the specific reaction rate, that is, the reaction rate per unit concentration of oxygen. Often the use of the absolute rate is valid because the only difference between the two plots is an additive factor, the logarithm of the concentration, which is often such a slowly varying function of temperature that the effect on the slope of the plot is negligible. However, for this case the concentration at the reacting surface, C_o, is shown by equation (8) to be an exponential function of temperature, which means that any valid Arrhenius plot must consider it. In addition, C_o is a function of the activation energy itself, which makes a valid Arrhenius plot

determination of the activation energy impossible. Thus, if the general form of the Arrhenius equation is to be useful, the method of application must be changed. The good agreement in values for the activation energy obtained by the use of equation (14), as well as the ability of the equation to account for the effects of diffusivity and flow velocity, indicates that, despite the simplifying assumptions contained in its derivation, the form of the equation, which is essentially an extension of the Arrhenius equation, is valid and that the equation is capable of correlating experimental data.

CONCLUSIONS

The following conclusions are drawn from the results of a study of the role of gaseous diffusion in the oxidation of metals:

1. Gaseous diffusion of oxygen to the metal surface is likely to be a rate-controlling factor in the oxidation of metals forming volatile oxides; this has been shown to be true for one such metal, molybdenum.

2. It is necessary to consider the effect of flow of gases over the metal surface in studying diffusion-controlled reactions.

3. The Arrhenius plot does not, and cannot be expected to, give accurate values for the activation energy of a diffusion-controlled reaction.

4. An equation has been derived which is essentially an extension of the simple Arrhenius equation to account for the effects of gaseous diffusion and which yields self-consistent values for the activation energy.

Langley Research Center,
National Aeronautics and Space Administration,
Langley Field, Va., November 2, 1959.

REFERENCES

1. Hampel, Clifford A., ed.: Rare Metals Handbook. Reinhold Pub. Corp. (New York), 1954.

2. Laidler, Keith J.: Chemical Kinetics. McGraw-Hill Book Co., Inc., 1950.

3. Carpenter, L. G.: The Kinetics of the Chemical Reaction Between a Solid and a Gas Stream Moving Over It. Tech. Note. Met. 182, British R.A.E., Oct. 1953.

4. Menzel, Donald H., ed.: Fundamental Formulas of Physics. Prentice-Hall, Inc., 1955.

5. Gilliland, E. R., and Sherwood, T. K.: Diffusion of Vapors into Air Streams. Industrial and Engineering Chemistry, vol. 26, no. 5, May 1934, pp. 516-523.

6. Sherwood, T. K., and Gilliland, E. R.: Diffusion of Vapors Through Gas Films. Industrial and Engineering Chemistry, vol. 26, no. 10, Oct. 1934, pp. 1093-1096.

7. Simnad, M., and Spilners, Aija: Kinetics and Mechanism of the Oxidation of Molybdenum. Jour. Metals, vol. 7, no. 9, sec. 2, Sept. 1955, pp. 1011-1016.

TABLE I.- WEIGHT LOSS DATA

(a) Series 1; air; volumetric flow, 0.12 std. cu ft/min

T, ^{o}R	u_{∞}, ft/sec	k, lb-ft^{-2}-sec^{-1}	Specimen dimension	Time, sec	Weight, g
1925	1.17	0.456×10^{-3}	0.98 inch by 0.45 inch	0 19 39 56 77 104 126	1.1908 1.1674 1.1413 1.1186 1.0908 1.0567 1.0298
2000	1.21	0.738×10^{-3}	0.98 inch by 0.45 inch	0 23 39 55 81 109	1.1842 1.1298 1.1028 1.0490 1.0158 .9588
2110	1.28	0.992×10^{-3}	0.98 inch by 0.45 inch	0 12 25 40 55 87 106 136	1.1720 1.1382 1.1023 1.0600 1.0178 .9246 .8789 .7990
2245	1.36	1.11×10^{-3}	0.98 inch by 0.45 inch	0 13 32 65 83 95	1.1368 1.0929 1.0326 .9288 .8746 .8393
2380	1.44	1.21×10^{-3}	0.98 inch by 0.45 inch	0 18 34 64 78 91	1.1460 1.0849 1.0319 .9298 .8840 .8382
2465	1.50	1.27×10^{-3}	0.98 inch by 0.45 inch	0 14 27 60 72 84 95	1.1258 1.0758 1.0288 .9116 .8626 .8230 .7815
2565	1.56	1.36×10^{-3}	0.98 inch by 0.45 inch	0 16 29 52	1.1184 1.0584 1.0112 .9231
2675	1.62	1.66×10^{-3}	0.98 inch by 0.45 inch	0 28 41	1.0228 .8910 .8314
2685	1.63	1.61×10^{-3}	0.98 inch by 0.45 inch	0 17 45 58 72	1.1342 1.0546 .9346 .8733 .8120
2725	1.65	1.73×10^{-3}	0.98 inch by 0.45 inch	0 21 54 67	1.1105 1.0097 .8430 .7860

TABLE I.- WEIGHT LOSS DATA - Continued

(b) Series 2; air; flow = 0.23 std. cu ft/min

T, ^{o}R	u_{∞}, ft/sec	k, lb-ft^{-2}-sec^{-1}	Specimen dimensions	Time, sec	Weight, g
2005	2.33	0.954×10^{-3}	0.97 inch by 0.45 inch	0 14 29 39 50 61 88 105	1.1730 1.1328 1.0928 1.0638 1.0337 1.0015 .9258 .8810
2040	2.37	1.03×10^{-3}	0.97 inch by 0.45 inch	0 25 37 48	1.1460 1.0736 1.0396 1.0060
2065	2.40	1.08×10^{-3}	0.97 inch by 0.45 inch	0 21 35 54 85 111	1.1862 1.1228 1.0782 1.0216 .9229 .8440
2200	2.56	1.13×10^{-3}	0.97 inch by 0.45 inch	0 16 27 40 50 74 95	1.1674 1.1140 1.0762 1.0342 1.0000 .9219 .8546
2215	2.58	1.09×10^{-3}	0.97 inch by 0.45 inch	0 14 27 54 62 80 92 107	1.1064 1.0644 1.0212 .9346 .9025 .8542 .8180 .7716
2315	2.69	1.29×10^{-3}	0.97 inch by 0.45 inch	0 17 37 63 79	1.1647 1.1005 1.0264 .9282 .8716
2365	2.75	1.33×10^{-3}	0.97 inch by 0.45 inch	0 13 37 58 74	1.1466 1.1005 1.0087 .9269 .8677
2425	2.82	1.30×10^{-3}	0.97 inch by 0.45 inch	0 13 26 41	1.1566 1.1068 1.0614 1.0048
2495	2.90	1.54×10^{-3}	0.97 inch by 0.45 inch	0 12 27 51 68	1.1366 1.0849 1.0200 .9098 .8356
2585	3.01	1.80×10^{-3}	0.97 inch by 0.45 inch	0 10 19 46 57 68	1.1260 1.0800 1.0322 .8930 .8358 .7788
2610	3.04	1.99×10^{-3}	0.97 inch by 0.45 inch	0 17 40 51	1.1276 1.0295 .8980 .8336
2660	3.10	2.01×10^{-3}	0.97 inch by 0.45 inch	0 20	1.0448 .9374

TABLE I.- WEIGHT LOSS DATA - Continued

(c) Series 3; air; volumetric flow = 0.315 std. cu ft/min

T, ^{o}R	u_{∞}, ft/sec	k, lb-ft^{-2}-sec^{-1}	Specimen dimensions	Time, sec	Weight, g
1945	3.10	0.912×10^{-3}	0.97 inch by 0.55 inch	0 13 26 54 64 84 98	1.3116 1.2702 1.2200 1.1400 1.1095 1.0432 1.0010
2065	3.29	1.18×10^{-3}	0.97 inch by 0.45 inch	0 11 26 40 63 79 91	1.1400 1.1056 1.0528 1.0040 .9282 .8724 .8356
2160	3.44	1.28×10^{-3}	0.97 inch by 0.49 inch	0 13 26 39 53 91	1.2104 1.1566 1.1056 1.0520 .9998 .8506
2225	3.55	1.25×10^{-3}	0.97 inch by 0.45 inch	0 25 39 59 71 87	1.1468 1.0570 1.0062 .9360 .8962 .8438
2340	3.73	1.31×10^{-3}	0.97 inch by 0.45 inch	0 11 24	1.1623 1.1130 1.0565
2430	3.87	1.46×10^{-3}	0.97 inch by 0.45 inch	0 11 23 33 57 71 81	1.1374 1.0925 1.0434 1.0002 .8988 .8440 .8010
2465	3.93	1.44×10^{-3}	0.97 inch by 0.45 inch	0 14 36	1.1482 1.0912 1.0002
2520	4.02	1.70×10^{-3}	0.97 inch by 0.46 inch	0 12 24 45 57	1.1322 1.0730 1.0160 .9072 .8496
2565	4.09	1.94×10^{-3}	0.97 inch by 0.45 inch	0 14 35 45 55	1.1046 1.0290 .9090 .8594 .8060
2620	4.18	2.08×10^{-3}	0.97 inch by 0.45 inch	0 22 34	1.0375 .9090 .8590

TABLE I.- WEIGHT LOSS DATA - Continued

(d) Series 4; 21.5 percent O_2, 78.5 percent He; flow = 0.284 std. cu ft/min

T, ^{o}R	u_{∞}, ft/sec	k, lb-ft^{-2}-sec^{-1}	Specimen dimensions	Time, sec	Weight, g
2200	3.16	1.79×10^{-3}	0.96 inch by 0.47 inch	0 12 22	1.1540 1.0864 1.0320
2350	3.38	1.81×10^{-3}	0.93 inch by 0.47 inch	0 11 36 47 55	1.0774 1.0190 .8918 .8360 .7940
2393	3.44	1.93×10^{-3}	0.97 inch by 0.53 inch	0 12 27 36	1.2473 1.1641 1.0720 1.0194
2451	3.52	2.12×10^{-3}	0.94 inch by 0.45 inch	0 11 28 38	1.0708 1.0078 .9075 .8508
2512	3.61	2.39×10^{-3}	0.94 inch by 0.45 inch	0 24	1.0475 .8917
2660	3.82	2.92×10^{-3}	0.95 inch by 0.45 inch	0 21 33	1.0496 .8744 .7846

TABLE I.- WEIGHT LOSS DATA - Concluded

(e) Series 5; 13.6 percent O_2, 86.4 percent He;

volumetric flow = 0.438 std. cu ft/min

T, ^{o}R	u_∞, ft/sec	k, lb-ft^{-2}-sec^{-1}	Specimen dimensions	Time, sec	Weight, g
2580	5.72	1.42×10^{-3}	0.95 inch by 0.45 inch	0 15 27 52 62	1.1140 1.0528 1.0056 .9098 .8714
2632	5.83	1.56×10^{-3}	0.94 inch by 0.45 inch	0 13	1.0592 1.0038
2771	6.14	2.19×10^{-3}	0.94 inch by 0.45 inch	0 25 37	1.0405 .8674 .7974
2812	6.23	2.12×10^{-3}	0.97 inch by 0.46 inch	0 12	1.1120 1.0384
2898	6.42	2.70×10^{-3}	0.97 inch by 0.46 inch	0 26	1.0503 .8564
2922	6.48	2.89×10^{-3}	0.95 inch by 0.45 inch	0 26	1.0457 .8382
2959	6.56	3.02×10^{-3}	0.95 inch by 0.45 inch	0 22	1.0022 .8393

TABLE II.- CALCULATED VALUES OF E_a AND P

Series	Gas composition	Calculations from exact equations for 2400° to 3000° R		E_a from Arrhenius plot, Btu/lb-mole		
		P	E_a, Btu/lb-mole	1900° to 2100° R	2100° to 2400° R	2400° to 3000° R
1	Air	2.48	36.7×10^3	22.1×10^3	7.38×10^3	20.2×10^3
2	Air	4.11	38.7	18.1	6.64	24.3
3	Air	6.40	39.4	19.4	5.73	29.7
4	21.5 percent O_2, 78.5 percent He	3.95	36.6	----------	3.7	19.7
5	13.6 percent O_2, 86.4 percent He	21.8	40.3	----------	----------	31.2
Mean value of E_a, Btu/lb-mole			38.3×10^3	19.9×10^3	5.88×10^3	25.0×10^3
Mean deviation, percent . . .			3.6	7.5	19.2	17.4

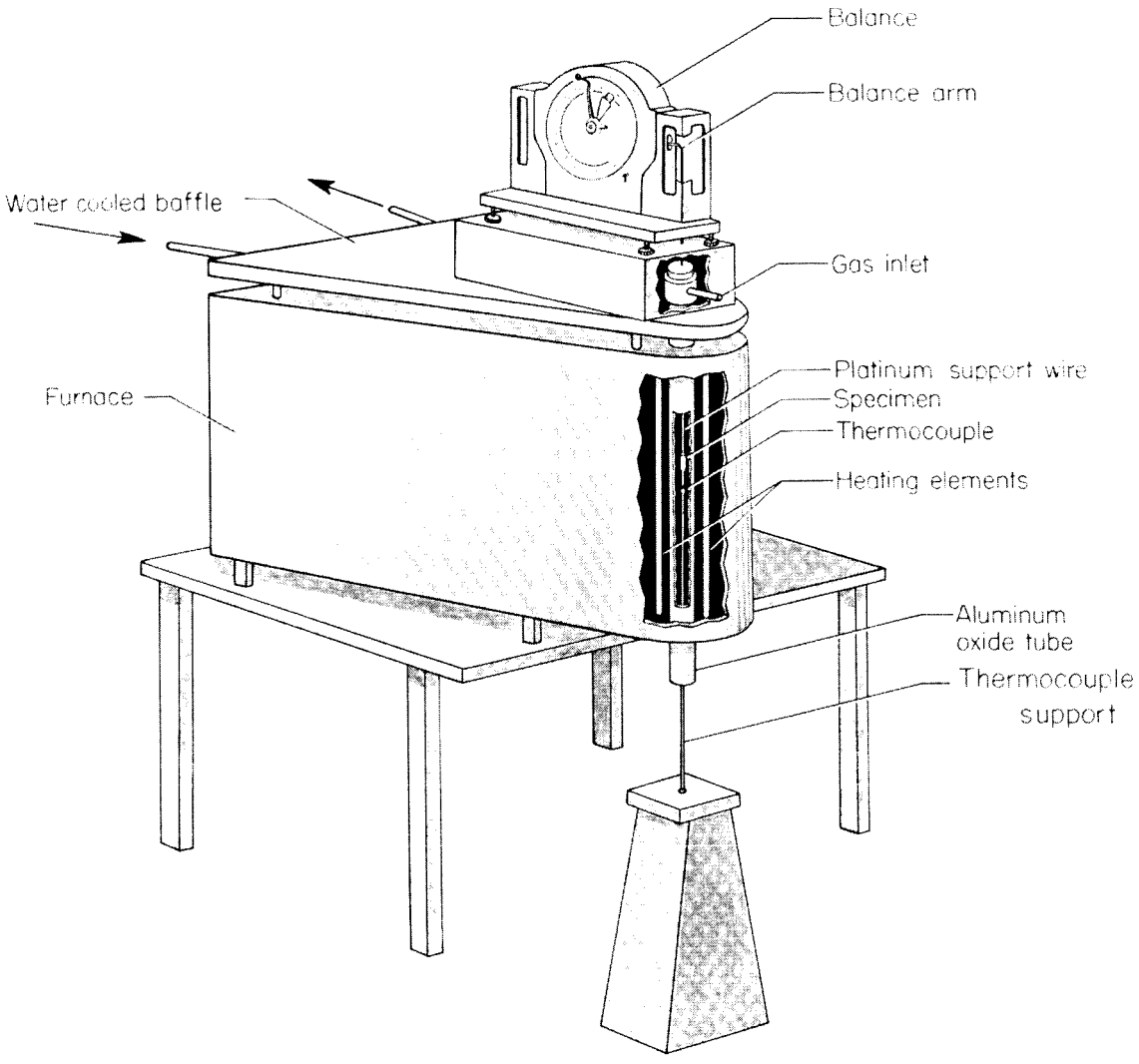

Figure 1.- Test setup.

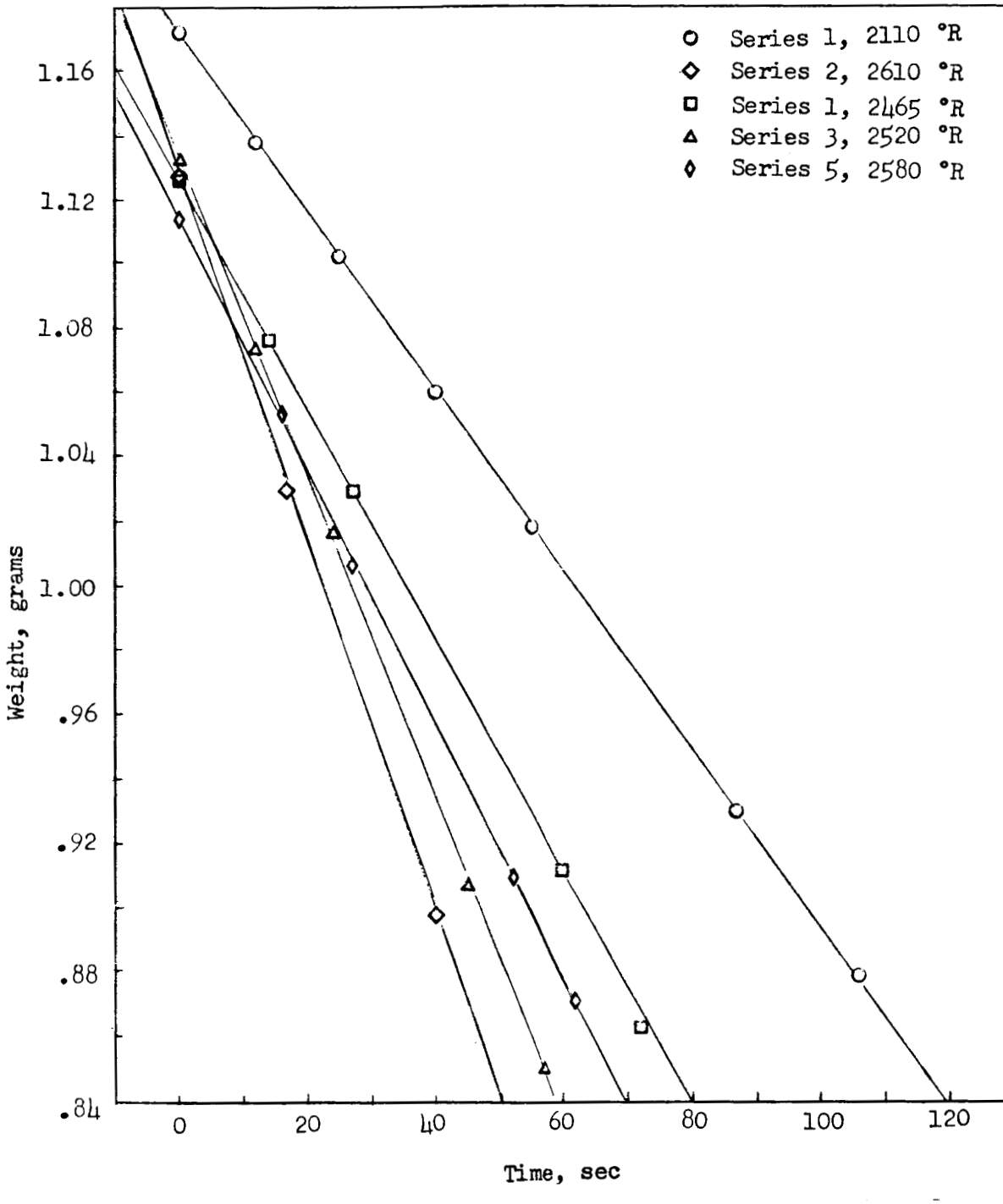

Figure 2.- Representative weight time curves.

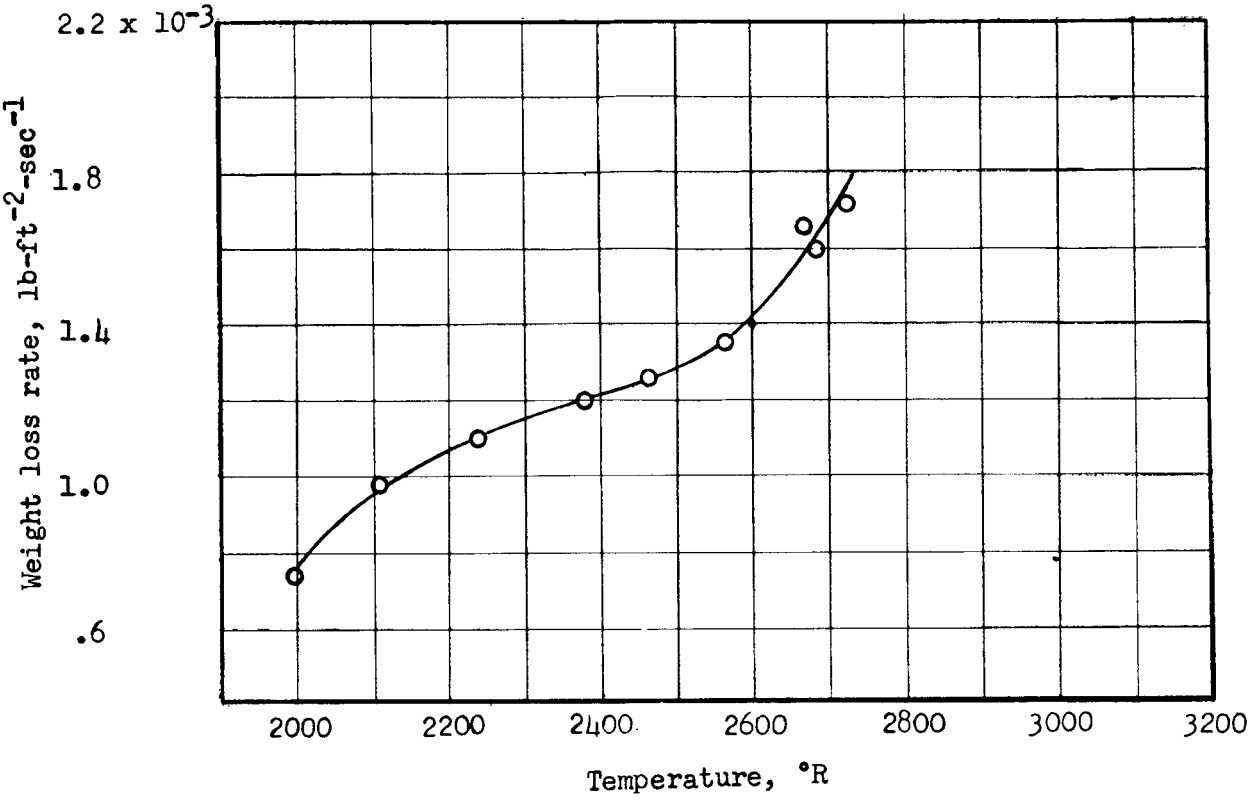

(a) Series 1; u_∞ = 1.17 to 1.65 ft/sec.

Figure 3.- Oxidation of molybdenum in air.

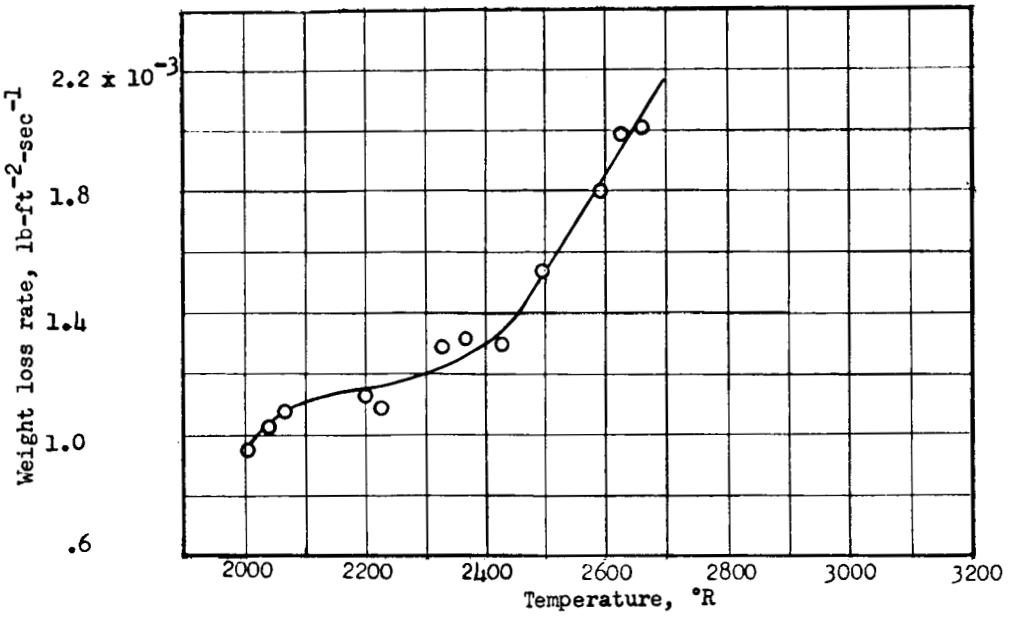

(b) Series 2; u_∞ = 2.33 to 3.10 ft/sec.

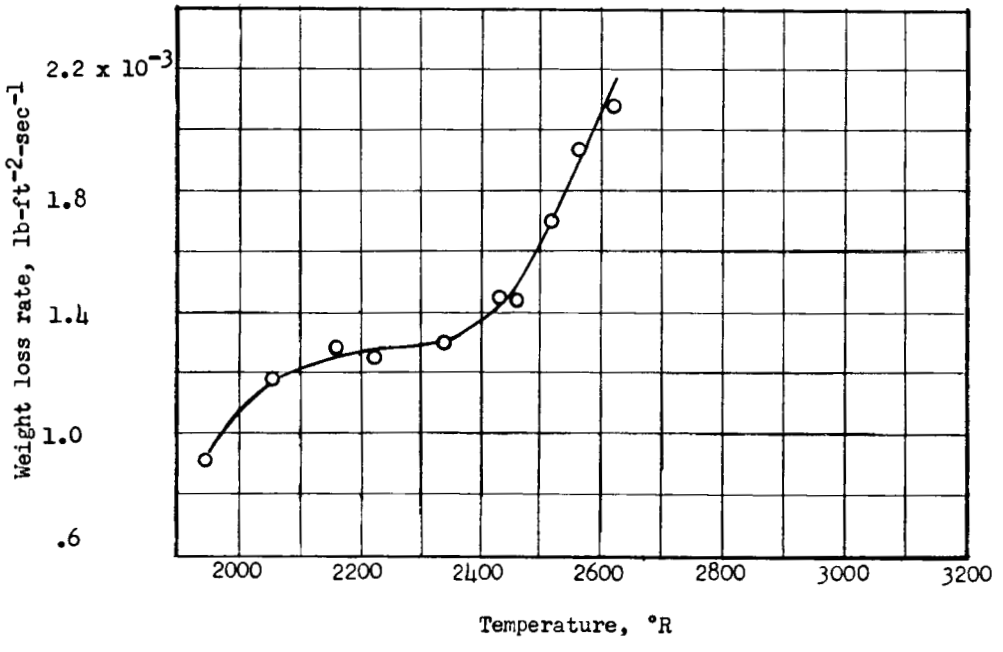

(c) Series 3; u_∞ = 3.10 to 4.18 ft/sec.

Figure 3.- Concluded.

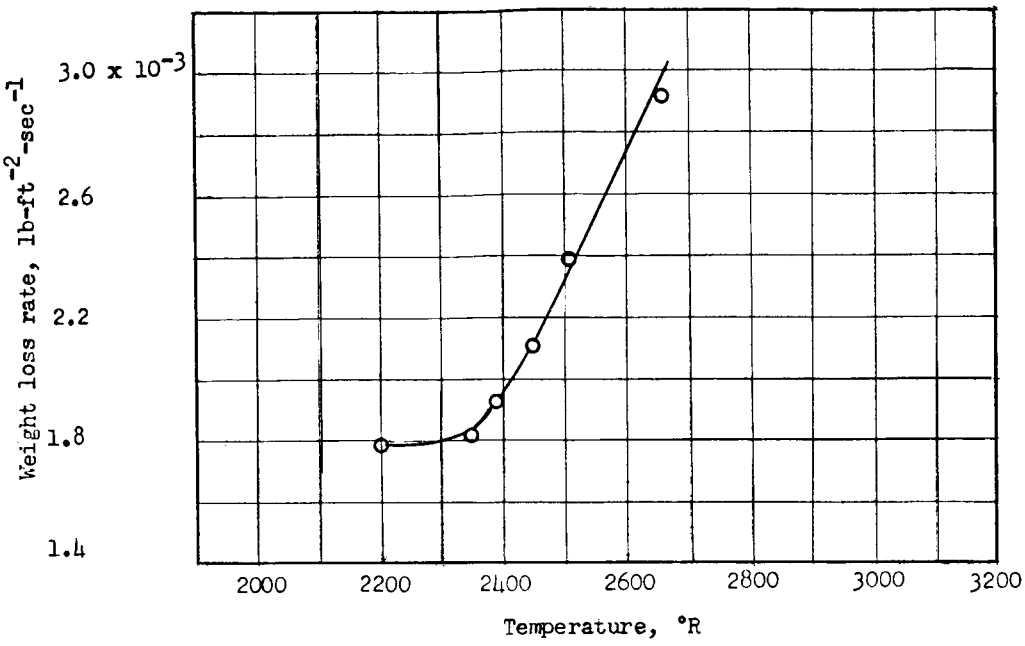

(a) Series 4; 21.5 percent O_2; 78.5 percent He; u_∞ = 3.16 to 3.82 ft/sec.

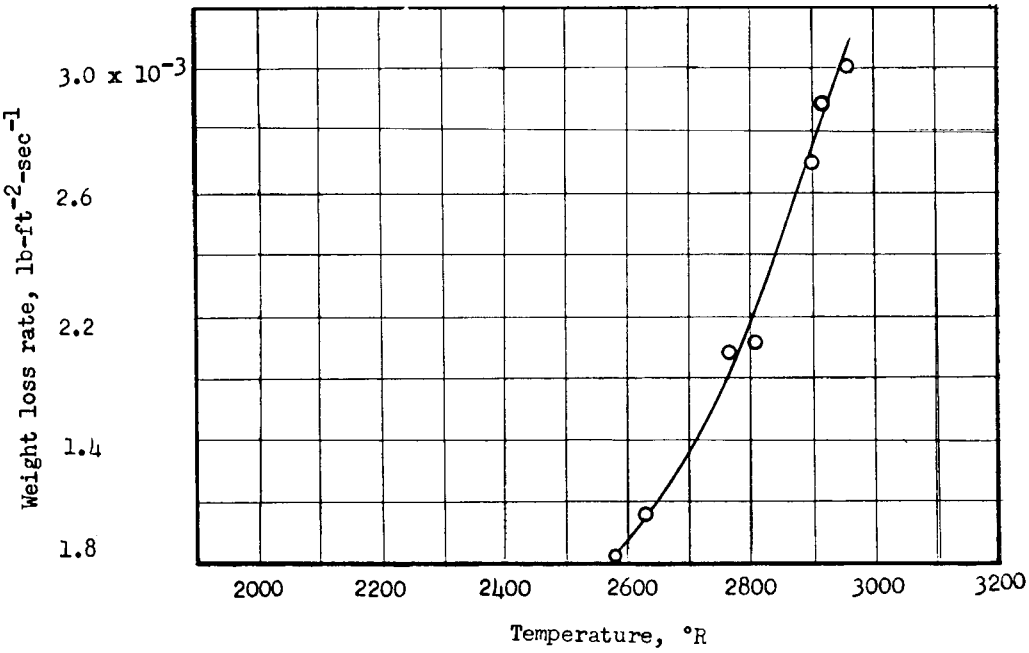

(b) Series 5; 13.6 percent O_2; 86.4 percent He; u_∞ = 5.72 to 6.56 ft/sec.

Figure 4.- Oxidation of molybdenum in helium-oxygen mixtures.

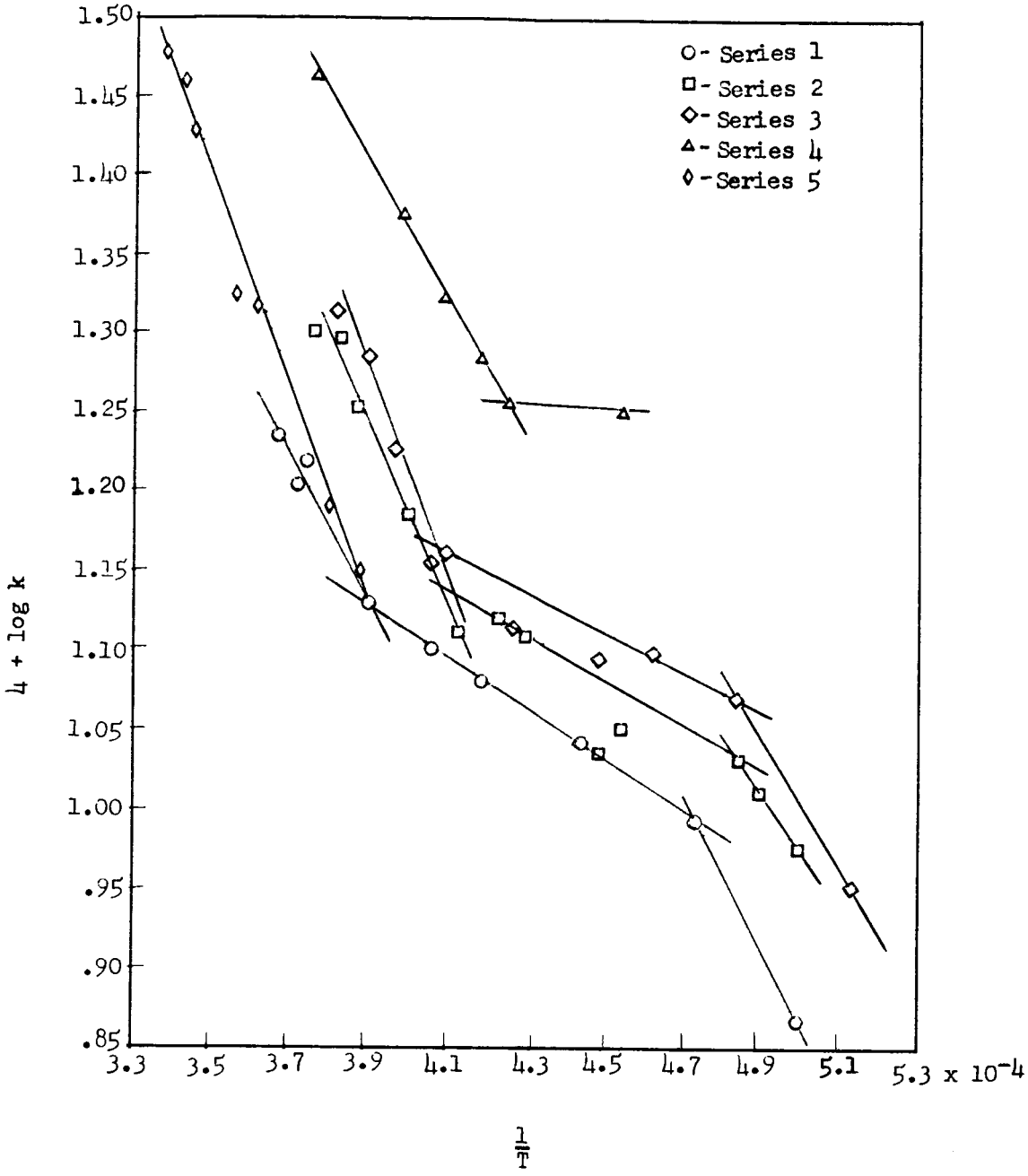

Figure 5.- Arrhenius plot of oxidation data.